
Rethinking Distributional Matching Based Domain Adaptation

Bo Li^{1‡}, Yezhen Wang^{23‡}, Tong Che^{4‡}, Shanghang Zhang^{1‡},
Sicheng Zhao¹, Pengfei Xu², Wei Zhou, Yoshua Bengio⁴⁵, Kurt Keutzer¹
¹UC, Berkeley ²DiDi, ³UC, San Diego
⁴MILA, Université de Montréal, ⁵CIFAR

Abstract

Domain adaptation (DA) is a technique that transfers predictive models trained on a labeled source domain to an unlabeled target domain, with the core difficulty of resolving distributional shift between domains. Currently, most popular DA algorithms are based on distributional matching (DM). However in practice, realistic domain shifts (RDS) may violate their basic assumptions and as a result these methods will fail. In this paper, in order to devise robust DA algorithms, we first systematically analyze the limitations of DM based methods, and then build new benchmarks with more realistic domain shifts to evaluate the well-accepted DM methods. We further propose InstaPBM, a novel Instance-based Predictive Behavior Matching method for robust DA. Extensive experiments on both conventional and RDS benchmarks demonstrate both the limitations of DM methods and the efficacy of InstaPBM: Compared with the best baselines, InstaPBM improves the classification accuracy respectively by 4.5%, 3.9% on Digits5, VisDA2017, and 2.2%, 2.9%, 3.6% on DomainNet-LDS, DomainNet-ILDS, ID-TwO. We hope our intuitive yet effective method will serve as a useful new direction and increase the robustness of DA in real scenarios. Code will be available at anonymous link: InstaPBM-RobustDA.

1 Introduction

Recent deep learning algorithms suffer from a fundamental problem: models require large-scale labeled training data and fail to generalize well to unlabeled new domains. With deep neural networks' capability to learn rich representations, recent domain adaptation methods attempt to solve this problem by matching the source and target distributions in representation space [1, 2, 3, 4, 5, 6, 7, 8, 9, 10, 11]. However, distributional matching (DM) cannot guarantee good generalization on the target domain and can even degrade results under realistic shifts [12, 13]. Some recent works [14, 12, 13, 15] propose modified versions of distributional matching that resolve label distribution shift [13] between domains. Although these alternatives can deal with some more general domain shifts, the domain shifts in the real world are still more complicated than commonly assumed, for we cannot restrict the variance, confounding factors, or peculiarities [16, 17] in target domain. Here we would like to take a step back and rethink the DM methods: is it always helpful for domain adaptation to match source and target distributions?

Following this motivation, we first discuss the limitations of DM algorithms under realistic domain shifts (RDS) in Sec. 2. For quantitatively analysis, we propose three representative RDS benchmarks in Sec. 3 and provide extensive empirical evaluations in Sec. 5 to support our analysis. Given the observation that DM methods are not robust in tackling RDS, we rethink UDA from first principles

[‡]These authors contributed equally to this work.

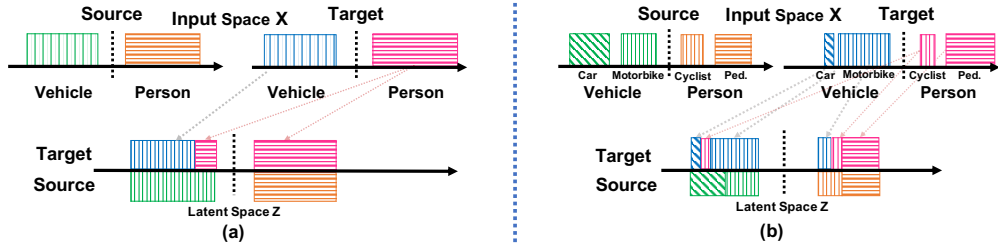


Figure 1: Failure cases of DM methods RDS. Colors denote categories, fill patterns denote sub-types, ped. denotes *pedestrians*.

and investigate the per-instance predictive behavior across domains. We believe a robust DA algorithm should be designed to deal with complexity and diversity in the real world. To promote robust DA algorithms on realistic domain shifts, we argue that one should not rely on DM methods whose performance are heavily affected by certain assumptions. Instead of matching distributions, we should directly match certain functional properties of a good predictor $p_\theta(y|x)$ that holds both in the source and target domains. We call the set of these properties "predictive behaviors". Since these predictive behaviors are about properties of the discriminative model $p_\theta(y|x)$, they add minimal assumptions to the distributions $p_S(x)$ and $p_T(x)$, leading to robustness in most cases. Following this idea, we propose a novel method: Instance-based Predictive Behavior Matching (InstaPBM) in Sec.4. Overall, InstaPBM consists of: (1) Mutual Information Predictive Behavior Matching; (2) Contrastive Predictive Behavior Matching; (3) Mix-up Predictive Behavior Matching. Each part corresponds to one predictive behavior we identify for a good predictive model on both domains.

The contributions of this paper are summarized as follows:

- We systematically analyze limitations of DM methods when tackling realistic domain shifts.
- We propose RDS benchmarks and extensively evaluate DM methods to verify their limitations.
- We further propose InstaPBM to contrastively match predictive behavior across domains and achieve robust DA under RDS.
- Extensive experiments on both conventional and RDS benchmarks demonstrate the efficacy of InstaPBM, which consistently outperforms the state-of-the-art methods by large margin: Compared with the best baselines, InstaPBM improves the classification accuracy respectively by 4.5%, 3.9% on Digits5, VisDA2017, and 2.2%, 2.9%, 3.6% on DomainNet-LDS, DomainNet-ILDS, ID-TwO. On RDS benchmarks, InstaPBM shows stronger robustness to realistic shifts compared with DM methods.

2 Limitations of Distributional Matching based DA

Notations and Setup. In this paper we focus on the unsupervised domain adaptation (UDA) and take classification problem as a running example. We use \mathcal{X} and \mathcal{Y} to denote the input and output space respectively, and \mathcal{Z} for the representation space generated from \mathcal{X} by a feature transformation $g : \mathcal{X} \mapsto \mathcal{Z}$. Following, we denote a labeling function $h : \mathcal{Z} \mapsto \mathcal{Y}$ and a composite predictive transformation $f = g \circ h : \mathcal{X} \mapsto \mathcal{Y}$. Specifically, f, g, h are parametrized by θ, ϕ, ψ , respectively. We use X, Y, Z as random variables from space $\mathcal{X}, \mathcal{Y}, \mathcal{Z}$, respectively. In the setting of unsupervised domain adaptation, we have access to labeled source data $(x, y) \sim \mathcal{P}_S(X, Y)$ and unlabeled target data $x \sim \mathcal{P}_T(X)$, where S and T denote source and target domain.

Distributional matching (DM) is a core component in most recent UDA methods where they use either domain adversarial classifier [18, 14, 19, 20, 21, 22, 23] or discrepancy-based approaches [8, 24, 25, 26]. In short, the purpose of distributional matching is to learn a shared feature representation space \mathcal{Z} and a feature transformation $g : \mathcal{X} \rightarrow \mathcal{Z}$ such that $\mathcal{P}_u(Y|X) = \mathcal{P}_u(Y|Z = g(X))$, $u \in \{S, T\}$. To achieve domain adaptation, many algorithms focus on minimizing the source domain errors and the distance between source and target distributions in the latent space:

$$\min_{\phi, \psi} L_S(\phi, \psi) + D(\mathcal{P}_S(Z) || \mathcal{P}_T(Z)) + \Omega(\phi, \psi) \quad (1)$$

where ϕ and ψ denote the parameters of g and h , D is a distance metric of distributions, $Z = g(X)$, and Ω is a regularizer term. Conventional instantiations of D can be Maximum Mean Discrepancy [27], domain classifier with Jensen-Shannon (JS) divergence [3] or Wasserstein distance [28]. Other generative or translation based DA [10, 11] can also be included in this framework as they match distribution $\mathcal{P}_T(X)$ and $\mathcal{P}_S(X)$ over pixel space \mathcal{X} instead of representation space \mathcal{Z} . To this end, we can induce the most common hypothesis of DM: $\mathcal{P}_S(Z) = \mathcal{P}_T(Z)$, $Z = g(X)$.

First, we prove that if the distributions of source domain and target domain are disjointed (which is most common case for high dimensional data such as images), then there is no guarantee for target label correctness even with a perfect distributional matching of representations. Specifically, for any arbitrary wrong label matching, there is a distributional matching which perfectly matches the representation, but wrongly matches labels in a way specified by the wrong label matching. This result tells us matching distributions is not sufficient for correctly matching labels between two domains. We detailed this into supplementary material due to space limitation.

Besides this theoretical results, exact matching distributions over representation space \mathcal{Z} will result in incorrect matches when $\mathcal{P}_S(Y) \neq \mathcal{P}_T(Y)$ and lead to unbounded target errors. We call this case label distributional shift (LDS [13, 15]). Consider the case of binary classification with non-overlapping support. Suppose the source contains 50% vehicle and 50% person, while the target contains 70% vehicle and 30% person. Successfully aligning these distributions in representation space requires the classifier to predict the same fraction of vehicle and person on source and target. If one achieves 100% accuracy on the source, then target accuracy will be at most 80% as illustrated in Fig. 1(a). Our experimental results in Sec. 5 also demonstrate this issue under LDS.

To tackle label distribution mismatch, another DM hypothesis: $\mathcal{P}_S(Z|Y = y) = \mathcal{P}_T(Z|Y = y)$, $\forall y \in \mathcal{Y}$ is proposed alongside [15]. However, such hypothesis may fail in the presence of intermediate layer distribution shift (ILDS), which indicates the intra-class feature distribution $P(Z|Y)$ may be different in two domains. A special case of ILDS is the sub-label distribution shift, where the distributions of sub-classes are different between source and target. Take the classification between *vehicle* and *person* as an example. Assume the source *vehicle* class contains 50% *car* and 50% *motorcycle*, while the target *vehicle* class contains 10% *car* and 90% *motorcycle*. Aligned with our analysis for LDS, since there are much higher proportion of *motorcycle* class in target, a perfect conditional classifier trained on uniformed source domain will be biased to the source sub-label distribution and mis-predict the extra amount of target *motorcycle* to another category: *person*, as illustrated in Fig. 1(b). Such phenomenon usually happens when the divergence between sub-classes (intra-class gap) is ‘‘larger’’ than the inter-class gap.

Another recent DM method [13] attempts to address LDS by asymmetrically relaxing the distribution alignment with hypothesis: $\frac{\mathcal{P}_T(Z)}{\mathcal{P}_S(Z)} \leq 1 + \beta$ for some $\beta > 0$. Such method proposes a relaxed distance for aligning data across domains that can be minimized without requiring latent-space distributions to match exactly. Even though the asymmetrical relaxation of distribution alignment mitigates the limitations of domain-adversarial algorithms [18, 14] under LDS, it is not sufficient for justification and suffers from the following issues: (1) To learn correct matching, one may have to select large β , making the objective itself too loose to learn discriminative target representations. (2) There may be some samples from target lying outside the support of source in the latent space, in which case the density ratio $\frac{\mathcal{P}_T(Z)}{\mathcal{P}_S(Z)}$ is unbounded, and the upper bound of target risk becomes vacuous. We name this case Target with Outliers(TwO). (3) Although the perfect alignments exist, there may also be other alignments that satisfy the objective but predict poorly on the target data.

In general, these hypotheses demonstrate the purpose of most DM methods’ theoretical study and algorithms. While they can make the performance guarantees vacuous under RDS, thus, we conclude that to achieve robust DA, we must devise DA algorithms without assuming any previously mentioned assumptions. We show how to devise such an algorithm in Sec. 4.

3 Realistic Domain Shift Benchmarks

In order to quantitatively verify the analysis of realistic domain shifts which limit the performance of DM methods in Sec. 2, we propose new DA benchmarks with three types of RDS, which better reflect the real world scenarios and can promote UDA research with more practical effectiveness:

Label Distribution Shift (LDS). LDS indicates the mismatch between source and target label distributions. We insert LDS on public datasets Digits5 [29] and DomainNet [30] by sampling target domain into long-tailed distribution among all classes (source domain unchanged). In this case, we do not require the source and target domains share the same visual looking in the same class, which is more aligned with real-world scenarios.

Intermediate Layer Distribution Shift (ILDS). ILDS indicates the intra-class feature distributions $P(Z|Y)$ are different in two domains, whose special case is sub-label distribution shift. We create ILDS on a public DA dataset DomainNet [30] by combining the similar sub-classes into corresponding meta-class and adjusting the number of samples for each sub-class to form long-tailed distribution within each meta-class on the target (source domain unchanged).

Target with Outliers (TwO). TwO indicates the target domain contains some samples that lie outside the support of source domain in the latent space \mathcal{Z} . To build such benchmark, we choose ImageNet as source and DomainNet as target, and add noisy data samples into the target.

Due to space limitation, we will provide more details about label, sub-label distributions on each dataset and examples of TwO in the supplementary material.

4 Instance-based Predictive Behavior Matching

Based on the analysis in Sec. 2 and Sec. 3, DM methods are susceptible to more realistic domain shifts. To overcome these limitations, we propose an Instance-based Predictive Behavior Matching (InstaPBM) method to match the instance predictive behaviors (PBs) across domains. PBs are about the intrinsic properties of the predictive model $p_\theta(y|x)$ which are independent of small perturbations of underlying source and target distributions, so they do not rely on strong assumptions of underlying distributions, this is why training domain-adapted classifier by matching PBs can achieve robustness. For consistent PB matching, we first propose to utilize mutual information maximization (MIM) on target data to simulate the mutual information change in the source domain. We further propose contrastive PB matching and mix-up PB to match different kinds of predictive patterns on both domains. To this end, we design a set of operations \mathcal{T} , which can be divided into two sets: (1) Semantic Preserving Operations \mathcal{T}_{sp} . (2) Mix-up Interpolation Operations \mathcal{T}_β . (3) Semantic Transforming Operations \mathcal{T}_{st} . (see Sec. 4.2 4.3 and 4.4). Other predictive behaviors matching may also be proposed, which we leave for future work.

4.1 Mutual Information Predictive Behavior Matching

Learning algorithms often construct predictors with supervised information. During training, the mutual information $I(X; Y)$ of source data increases progressively, because the back-propagated supervised information leads to a strong correlation between the predicted label and input data. We opine that the target domain should also obey this pattern (or predictive behavior). However, a challenge emerges since the target data is unlabeled. To this end, we propose to use mutual information maximization to simulate this behavior on target domain, which can be equivalently expressed as: $I_T(X; Y) = H_T(Y) - H_T(Y|X)$.

Therefore the objective of mutual information $I_T(X; Y)$ maximization is equivalent to two parts: maximizing the info-entropy $H_T(Y)$ and minimizing the conditional entropy $H_T(Y|X)$. Intuitively, by minimizing $H_T(Y|X)$ on unlabeled data, we increase the discriminability of the predictor towards target domain, which drives the decision boundary away from the target data [31]. However, when the groundtruth label distribution is imbalanced, minimizing $H_T(Y|X)$ solely can be trivially done by predicting a 100% probability on one particular class. Thus we need to maximize the $H_T(Y)$ in order to prevent output to collapse to a particular class, namely, ensure the diversity of the output [32]. It is worth noting that we do not expect $H_T(Y)$ to be as large as possible, instead, we maximize $H_T(Y)$ only when it is lower than a pre-defined threshold. The corresponding loss function is as follows:

$$\mathcal{L}_M(T; \theta) = \mathbb{E}_{y \sim \mathcal{P}_\theta(Y)}[\log p_\theta(y)] - \mathbb{E}_{x \sim \mathcal{P}_T(X)}[\sum_y p_\theta(y|x) \log p_\theta(y|x)] \quad (2)$$

where $p_\theta(y|x)$ denotes probability of each sample output from predictor, $\mathcal{P}_\theta(Y)$ represents the distribution of predicted target label Y . We use a moving average $q(y)$ of $p_\theta(y|x)$, $x \sim \mathcal{P}_T(x)$ as an

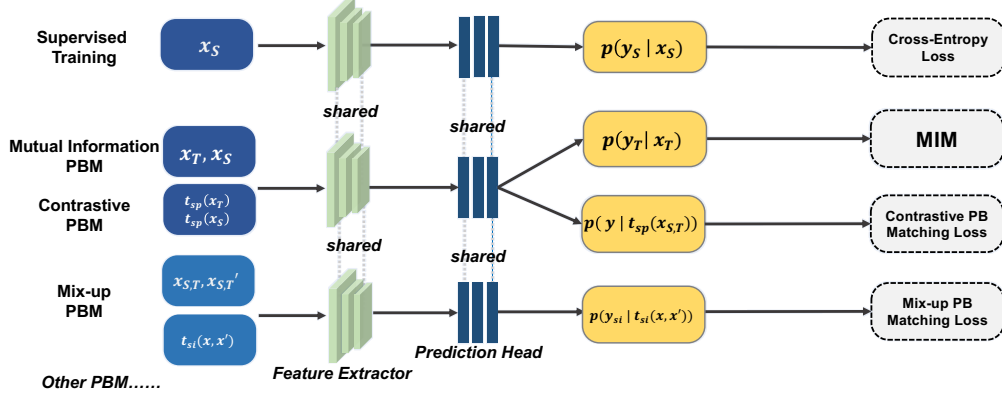


Figure 2: The proposed method of our InstaPBM, where $x_u \sim \mathcal{P}_u(X)$, $u \in \{S, T\}$ denote data from source and target domain, $t \sim \mathcal{T}_{sp}$ and $t \sim \mathcal{T}_{st}$ denote semantic preserving and semantic transforming operations respectively, y_{st} denote semantic transforming labels in self-supervise training.

approximation of $p_\theta(y)$. Then we estimate the gradient of $H_\theta(Y) = \mathbb{E}_{y \sim \mathcal{P}_\theta(Y)}[\log p_\theta(y)]$ as:

$$\tilde{\nabla} H_\theta(Y) = \sum_{(x,y) \sim \mathcal{P}_S} \nabla_\theta p_\theta(y|x) \log q(y) \quad (3)$$

4.2 Contrastive Predictive Behavior Matching

Another predictive behavior that should be satisfied on both domains is about "augmentation consistency". Consider t is an augmentation operation which preserves the semantics of the image X (e.g. color distortion), then t should not change the label of the image $t(X)$ after the operation. Here we introduce semantic preserving operations for CPBM, which will keep semantics of the instances. The predictive behavior we are matching using this loss can be described as "a good predictor on both domains should predict the same label for X and $t(X)$, while (with a high probability) predict different labels for X and X' when X and X' belong to different classes".

The semantic preserving \mathcal{T}_{sp} operations on instances include two types:(1) Random Augmentation [33]; (2) Noise Injection [34]. Following this idea, we propose an contrastive training loss to match the PB for instances before and after operations, and maximize the disagreement for instances from different classes. The model is jointly trained on source and target for the first objective and on the source for the second. Formally, the objective can be written as

$$\begin{aligned} \mathcal{L}_C(S, T; \theta) = & \mathbb{E}_{x \sim \mathcal{P}_{S,T}, t \sim \tau} [D_{KL}(p_\theta(y|x) || p_\theta(y|t(x)))] \\ & - \lambda_{con} \mathbb{E}_{(x,y) \sim \mathcal{P}_S, (x',y') \sim \mathcal{P}_S, y \neq y'} [D_{KL}(p_\theta(y|x) || p_\theta(y'|x'))] \end{aligned} \quad (4)$$

where x' and x belong to different classes. The training process can be divided into: (1) Apply a $t \sim \mathcal{T}_{sp}$ operation on input instance $x \sim \mathcal{P}_{S,T}$ from both domains to have the transformed version $t(x)$. Then feed $(x, t(x))$ into p_θ to compute $p_\theta(y|x)$ and $p_\theta(y|t(x))$. (2) Minimize KL divergence between the two distributions $D_{KL}(p_\theta(y|x) || p_\theta(y|x'))$. These operations advance the model with realistic augmented examples and create the same training objective of semantics maintaining [33], so that this predictive behavior is consistently strengthen across domains.

4.3 Mix-up Predictive Behavior Matching

Aligned with our predictive behavior matching objective, inspired by [35], we introduce Mix-up Predictive Behavior Matching (MuPBM) with linear interpolation operations $t(x, x', \beta) = \beta x + (1 - \beta)x' \sim \mathcal{T}_\beta$, $\beta \in [0, 1]$ where x, x' are raw input vectors sampled from both domains, and we create labels of $t(x, x', \beta)$ as $y_{si} = \beta y + (1 - \beta)y'$, $\beta \in [0, 1]$, where y, y' are one-hot label encodings in source domain and softmax probabilities output from predictor in target domain. The predictive behavior should remain identical on both domains with introduced operations \mathcal{T}_β . Namely, MuPBM ensures a smooth transition between classes and encourages the model to behave similarly on linear

interpolations of samples in both domain. Our objective enforces consistency and reduce undesirable oscillations by jointly training on both domains to deal with these *soft* linear interpolations. Formally, the objective can be written as Eq. 5, where $q(y_{si}|x, x')$ denotes distribution defined by interpolated softmax $y_{si} = \beta y + (1 - \beta)y'$.

$$\mathcal{L}_U(S, T; \phi, \psi) = \mathbb{E}_{(x, x') \sim \mathcal{P}_{S, T}, t \sim \mathcal{T}_{st}} [D_{KL}(p_\theta(y | t(x, x', \beta)) || q(y_{si}|x, x'))] \quad (5)$$

4.4 Other Predictive Behavior Matching

There has been some other works align with our intuition of PB matching [36, 37]. For example, introduced by [36], self-supervised tasks also describe a predictive behavior that should be identical between domains, which we call as Task-oriented Predictive Behavior Matching hereafter. Following [36], we apply three semantic transforming operations (*Rotation Prediction*, *Vertical Flip Prediction*, *Patch Location Prediction*) to realize this objective. We specify the operations as $t \sim \mathcal{T}_{st}$ and its self-supervised label $\tilde{y}_t = t(x_{S, T})$. We denote each corresponding auxiliary head as h_t parameterized by ω for each $t(x_{S, T})$, and obtain the following training objective with supervised loss function L_t :

$$\mathcal{L}_S(S, T; \phi, \omega) = \mathbb{E}_{x \sim \mathcal{P}_{S, T}, t \sim \mathcal{T}_{st}} [L_t(h_t \circ g(t(x_{S, T})), \tilde{y}_t)] \quad (6)$$

To summarize, InstaPBM investigated the potential of PB matching for robust DA. Additionally, it has the potential to add more PB matchings to further enhance robustness. The overall optimization is defined as in Eq. 7, where ω is the parameters of predictor h_t .

$$\min_{\theta, \phi, \omega} \lambda_M \mathcal{L}_M(S, T; \theta) + \lambda_C \mathcal{L}_C(S, T; \theta) + \lambda_U \mathcal{L}_U(S, T; \phi, \psi) + \lambda_S \mathcal{L}_S(S, T; \phi, \omega) \quad (7)$$

5 Experiments

We evaluate the limitations of DM based methods and the efficacy of InstaPBM on both conventional and RDS benchmarks. More experimental details are included in the supplementary material.

5.1 Experimental Settings

Conventional Benchmarks. We experiment on two common conventional DA benchmarks: Digits5 [29, 38, 39, 40] and VisDA2017 [41]. Digits5 consists of five vastly different domains: MNIST (MN), MNISTM (MM), USPS (US), SYNTH (SY), SVHN (SV). Each domain contains more than 50K images except USPS, which has about 10K images. VisDA2017 is a challenging testbed for UDA with domain shift from simulation to real, which has around 280K images from 12 classes.

Proposed RDS Benchmarks. We propose the following RDS benchmarks: (1) **Label Distribution Shift:** Digits5-LDS, VisDA2017-LDS, and DomainNet-LDS by respectively resampling Digits5, VisDA2017, and DomainNet [30] under LDS protocol; (2) **Intermediate layer Distribution Shift:** DomainNet-ILDS by combining similar labels into a parental label on DomainNet; C, R, S, P, I, Q represent six subdomains: Clipart, Real, Sketch, Painting, Infograph and Quickdraw respectively. (3) **Target with Outliers:** ID-TwO by selecting 18 overlapped classes between the source ImageNet 1K and target DomainNet for close-set UDA. Due to space limitation, statistics of RDS benchmarks and results on VisDA2017-LDS and Digits5-LDS will be provided in supplementary material.

Baselines. We compare with the following state-of-the-art methods: DM methods: DANN [42], CoRAL [43, 44, 45], DAN [8], HoMM [26]; conditional DM: CDAN[14], sDANN- β [13], JAN [46]; none DM: ADR [47], SE [48] and CAN [49] on aforementioned benchmarks.

Implementation Details. We use LeNet, ResNet-101, and ResNet-101 as backbone networks for DA tasks on Digits5, VisDA2017, and DomainNet, respectively. We replace the last fully-connected (FC) layer with the task-specific FC layer. Please find more details in the supplementary material.

5.2 Results and Analysis

5.2.1 Conventional Benchmarks

Table 1 and Table 2 show the performance comparison on Digits5 and VisDA2017 respectively. From the results, we observe that: (1) The source-only method that directly transfers the model trained

Table 1: Performance comparison on **Digits5** dataset. Best accuracy in bold.

Method	MN				MM				US				SY				SV				Average
	MM	US	SY	SV	MN	US	SY	SV	MN	MM	SY	SV	MN	MM	US	SV	MN	MM	US	SV	
Source Only	67.7	73.9	54.2	47.3	81.8	73.4	50.9	50.7	75.6	50.9	42.5	41.6	85.2	65.0	82.1	75.6	56.8	44.8	63.2	73.2	62.8
DAN [8]	62.6	79.7	47.6	43.1	99.2	80.5	60.5	53.3	48.2	28.3	28.2	24.4	88.6	65.8	86.6	79.3	74.5	56.2	70.1	93.3	63.5
DANN [42]	64.9	75.0	52.3	42.5	89.0	71.3	49.7	58.6	67.1	53.7	45.3	40.1	81.3	63.6	79.0	83.2	70.2	55.5	63.2	77.5	64.2
CoRAL [44]	70.2	83.9	54.2	45.8	98.7	78.4	59.5	53.0	72.6	51.3	41.9	33.8	87.5	67.4	82.8	84.5	68.5	53.2	67.4	90.8	67.3
HoMM [26]	72.2	86.2	58.0	50.5	98.2	79.6	58.7	51.6	75.2	49.1	43.6	37.7	88.3	68.4	83.5	82.4	68.7	60.4	65.5	88.8	68.3
sDANN- β [13]	50.2	70.4	44.5	38.3	79.0	70.5	52.9	53.4	74.6	48.9	34.5	36.6	83.4	60.6	79.0	71.6	60.2	47.8	42.8	64.5	58.2
JAN [46]	66.2	88.5	47.9	47.7	98.4	80.8	59.6	54.2	68.8	32.6	38.1	32.2	87.2	57.7	83.0	79.9	71.5	52.9	69.8	90.8	65.4
CDAN [14]	75.7	85.5	65.5	54.0	99.0	79.7	62.6	56.1	69.0	51.3	46.3	38.4	89.6	71.8	84.6	83.4	73.8	58.2	72.0	91.4	70.4
CDAN+E [14]	70.7	90.8	63.4	49.3	99.5	88.5	73.1	63.5	87.0	46.8	46.2	34.0	86.0	65.4	67.0	80.5	81.5	62.7	71.8	95.9	71.2
CAN [49]	82.4	94.6	45.8	42.4	99.5	70.7	71.2	61.8	88.1	53.3	39.8	31.1	94.6	81.8	94.1	82.3	97.1	89.4	73.0	95.3	74.4
ADR [47]	83.6	93.4	58.8	50.1	99.6	84.9	72.6	37.3	48.6	43.4	38.6	37.6	97.0	84.1	94.6	81.9	83.4	88.1	73.8	97.6	72.5
SE [48]	81.7	94.2	38.7	34.7	99.4	85.4	90.1	60.1	88.2	53.6	36.4	30.0	95.0	83.2	91.3	80.7	77.2	87.2	67.4	95.4	73.5
InstaPBM(ours)	94.6	96.5	45.7	45.9	99.2	67.3	91.1	77.7	92.0	58.6	42.0	32.3	97.2	89.2	94.8	87.0	97.6	91.7	80.0	96.6	78.9

Table 2: Performance comparison on **VisDA2017** dataset. Best accuracy in bold.

Method	a-plane	bicycle	bus	car	horse	knife	m-cycle	person	plant	skb	train	truck	Average
Source Only	72.3	6.1	63.4	91.7	52.7	7.9	80.1	5.6	90.1	18.5	78.1	25.9	49.4
DANN [42]	81.9	77.7	82.8	44.3	81.2	29.5	65.1	28.6	51.9	54.6	82.8	7.8	57.4
DAN [8]	68.1	15.4	76.5	87.0	71.1	48.9	82.3	51.5	88.7	33.2	88.9	42.2	62.8
JAN [46]	75.7	18.7	82.3	86.3	70.2	56.9	80.5	53.8	92.5	32.2	84.5	54.5	65.7
MCD[50]	87.0	60.9	83.7	64.0	88.9	79.6	84.7	76.9	88.6	40.3	83.0	25.8	71.9
ADR [47]	87.8	79.5	83.7	65.3	92.3	61.8	88.9	73.2	87.8	60.0	85.5	32.3	74.8
SE [48]	95.9	87.4	85.2	58.6	96.2	95.7	90.6	80.0	94.8	90.8	88.4	47.9	84.3
CAN [49]	97.0	87.2	82.5	74.3	97.8	96.2	90.8	80.7	96.6	96.3	87.5	59.9	87.2
InstaPBM(ours)	95.4	86.3	94.0	93.1	92.8	95.6	92.2	87.5	92.8	85.5	92.4	85.0	91.1

on source to target performs the worst. This is reasonable, because it does not address the domain shift. (2) On DIGITS, InstaPBM achieves 4.5% performance gain as compared to the best baseline (*i.e.* CAN). Please note that many UDA methods [51, 36] only experiment on several selected scenarios (*e.g.* MNIST->SVHN, USPS->MNIST), which cannot sufficiently verify their efficacy and generalization. (3) On VisDA2017, InstaPBM obtains the best accuracy on average: 3.9% and 6.8% absolute improvements compared to the best baseline CAN [49] and the self-embedding (SE) [48], which wins the first place in VisDA-2017 leaderboard. Please note that we do not use any engineering trick (*e.g.* ensembling, parameters grid searching, warm-up, etc).

5.2.2 Realistic Domain Shift (RDS) Benchmarks

Label Distribution Shift (LDS). From the left part results in Table 3, we observe that: (1) Almost all DM methods have the detrimental effects on adaptation under LDS, which verifies their limitations analyzed in Sec. 2. (2) Conditional DM methods perform relatively better than DM methods, which demonstrates they are more robust to LDS. (3) None DM methods are least affected by LDS and InstaPBM performs the best, which indicates its strong resistance towards LDS.

Intermediate Layer Distribution Shift (ILDS). The right part in Table 3 shows the performance comparison on DomainNet-ILDS. Similar to LDS scenarios, the DM methods and none DM methods have a weak and strong resistance towards ILDS respectively. What differs from the results of LDS is that conditional DM methods also result in adaptation performance decay on ILDS Benchmarks. Our method still achieves the best result on ILDS Benchmarks as compared to all other baselines.

Target with Outliers (TwO). The result in Table 4 verifies our analysis that when target data are filled with outliers from other domains, DM will suffer interventions. None DM methods, such as our InstaPBM, are less affected since they do not rely on matching representation distributions. For outliers, we can better capture their semantics by contrastively matching predictive behaviors with source domain data per instance.

5.3 Ablation Study

Our approach has four main components: MIM, CPBM, MuPBM and TPBM. We conduct an exhaustive ablation study to explore the specific contribution of each component. The results on 7 different benchmarks are shown in Table 5. We have the following observations: (1) Comparing to

Table 3: Performance comparison on **DomainNet-LDS** and **DomainNet-ILDS** Benchmarks.

Method	LDS Benchmark							ILDS Benchmark						
	I->C	C->R	C->S	S->P	P->R	R->C	Average	I->C	C->R	C->S	S->P	P->R	R->C	Average
Source Only	31.2	52.5	46.3	39.9	53.7	49.0	45.4	40.9	62.3	58.9	49.0	64.7	60.4	56.0
DAN [8]	22.0	46.3	42.2	36.6	47.6	46.6	40.2	32.3	57.6	52.0	46.7	61.8	56.5	51.1
CoRAL [44]	22.5	47.1	44.6	38.3	49.3	46.3	41.3	35.2	60.1	53.8	49.2	63.0	59.1	53.4
HoMM [26]	21.5	47.8	45.2	38.5	48.4	47.7	41.5	37.2	61.2	55.9	50.2	58.6	61.3	54.1
DANN [42]	27.2	51.6	46.6	40.1	51.4	46.3	43.9	40.4	62.2	54.6	51.5	62.6	59.5	55.1
JAN [46]	24.7	50.3	43.1	37.4	49.3	48.2	42.2	38.4	60.5	55.4	46.6	58.6	59.9	53.2
CDAN [14]	30.0	53.2	46.9	41.4	54.3	48.0	45.6	37.4	59.5	53.2	46.7	61.3	56.5	52.4
sDANN- β [13]	32.0	52.1	47.2	45.2	50.3	49.7	46.1	39.1	60.2	53.5	47.2	60.4	60.1	54.2
CDAN+E [14]	29.7	55.3	48.1	42.4	54.3	53.2	47.2	38.6	61.6	53.9	45.9	62.8	58.6	53.6
CAN [49]	36.0	58.2	53.2	47.3	53.6	57.6	51.0	40.1	64.6	55.4	47.3	63.2	59.1	56.5
ADR [47]	34.5	54.6	47.7	42.3	56.6	51.3	47.8	43.2	65.4	57.1	51.4	66.8	58.0	57.0
SE [48]	33.6	56.6	50.3	40.6	55.5	55.1	48.6	45.3	67.2	61.3	52.4	70.0	66.3	60.4
InstaPBM(ours)	38.5	60.2	52.3	47.0	61.6	59.6	53.2	49.6	72.1	64.1	53.1	72.3	68.7	63.3

Table 4: Performance comparison on **ID-Two** based on ResNet-101. Best accuracy in bold.

Method	a-plane	bicycle	clock	dog	f-pan	lion	n-lace	potato	sock	b-ball	bucket	cup	d-bell	laptop	lipstick	panda	shark	w-bottle	Average
Source Only	52.8	69.5	67.9	61.2	51.6	56.3	94.0	30.2	53.7	46.8	57.5	59.9	61.3	57.3	55.0	47.8	45.7	59.8	57.1
DAN [8]	49.3	61.5	68.1	63.0	56.9	51.1	83.8	37.6	51.3	42.1	53.3	60.9	57.2	62.1	51.8	42.0	41.6	57.3	55.1
DANN [42]	56.7	82.0	76.3	62.7	51.3	54.4	88.1	35.7	55.7	43.7	72.1	57.0	63.3	57.5	54.6	43.6	44.4	59.8	58.8
HoMM [26]	54.0	75.9	68.1	59.8	53.2	57.9	93.1	36.2	55.4	54.1	73.1	58.4	68.1	67.7	54.8	46.5	57.2	62.1	60.9
CoRAL [44]	53.7	91.4	89.3	70.6	62.4	53.7	69.8	42.9	57.3	40.0	63.3	58.1	62.3	60.0	58.0	52.4	54.1	61.4	61.1
sDANN- β [13]	58.4	72.7	78.4	42.6	64.2	50.1	81.4	38.4	50.5	51.0	69.4	48.1	46.4	56.1	59.5	49.2	49.5	76.0	57.8
JAN [46]	53.7	69.7	76.5	62.6	67.2	55.1	85.2	40.4	56.5	51.1	71.9	50.1	64.4	65.5	56.5	44.7	47.5	68.0	60.4
CDAN [14]	55.5	87.0	73.2	62.5	61.6	54.9	83.3	59.6	58.6	53.5	74.2	70.0	69.3	69.2	56.8	44.6	77.4	74.0	65.8
CDAN+E [14]	55.8	76.5	77.4	70.7	61.6	58.4	89.6	47.6	61.4	61.1	75.4	67.1	81.9	71.1	55.3	46.1	52.9	78.6	66.0
CAN [49]	60.7	93.2	88.8	74.5	77.3	59.8	87.7	52.1	79.3	84.2	83.2	72.0	81.4	70.6	58.2	59.5	62.9	83.5	73.8
ADR [47]	57.7	85.8	82.1	73.5	73.0	62.7	87.5	52.6	73.6	68.2	79.4	67.5	79.6	77.3	53.1	55.1	52.1	77.3	69.9
SE [48]	58.3	83.9	84.9	71.3	73.5	65.0	86.7	53.1	77.6	74.0	81.5	71.4	77.8	74.3	56.3	57.7	55.3	81.4	71.3
InstaPBM(ours)	62.7	96.3	91.3	72.7	76.3	66.3	91.5	55.4	86.2	86.8	87.5	67.0	84.9	92.7	61.8	61.8	59.4	92.2	77.4

Table 5: Ablation study on different components in InstaPBM across all benchmarks.

Method	Conventional Benchmarks		RDS Benchmarks					Average
	VisDA2017	Digits5	V-LDS	D-LDS	DN-LDS	DN-ILDS	ID-Two	
Baseline	49.4	62.8	55.1	55.8	45.4	56.0	57.1	54.5
+MIM	83.5	72.1	69.8	64.3	52.9	61.1	73.8	68.2
+CPBM_RA	77.9	67.5	62.2	59.5	50.7	57.7	69.5	63.6
+CPBM_NI	71.2	65.7	63.3	57.1	48.1	56.7	65.1	61.0
+CPBM_ALL	79.2	70.2	64.5	60.4	50.9	59.0	69.9	64.9
+MuPBM	75.3	67.1	59.5	58.9	49.2	58.7	64.3	61.8
+TPBM_ROT	62.3	64.3	56.1	57.2	45.7	56.1	60.5	57.5
+TPBM_QDR	64.6	66.2	58.2	59.3	46.1	56.7	61.3	58.9
+TPBM_FLIP	59.8	62.6	55.9	54.3	45.5	56.2	58.3	56.1
+TPBM_ALL	65.5	67.3	58.5	60.0	46.5	57.7	61.8	59.6
+InstaPBM	91.1	78.9	74.7	66.2	53.2	63.3	77.4	72.1

Baseline denotes model trained on source without adaptation. **+MIM** denotes using our mutual information maximization objective. **+MuPBM** represents Mix-up Predictive Behavior Matching. **+CPBM_*** denotes applying Contrastive Predictive Behavior Matching by Random Augmentation(RA), Noise Injection(NI) and both(ALL) specifically. **+TPBM_*** denotes implementing Task-oriented Predictive Behavior Matching by using different self-supervised tasks(i.s. Rotation Prediction(ROT), Vertical Flip Prediction(FLIP) and Patch Location Prediction(QDR)). **V-LDS** denotes **VisDA2017-LDS**, **D-LDS** denotes **Digits5-LDS**, **DN-LDS** and **DN-ILDS** denote **DomainNet-LDS** and **DomainNet-ILDS** respectively. **InstaPBM** denotes the integration of MIM, MuPBM, CPBM_ALL and TPBM_ALL.

Source Only method, each proposed component(From 2 to 10 rows) can improve the classification accuracy on all benchmarks, which demonstrates that these components can not only improve the domain adaptation performance but also have a strong resistance towards RDS; (2) Among all these components, MIM obtains the highest performance improvement (13.7%) followed by CPBM_ALL (10.4%); (3) MIM, CPBM, MuPBM and TPBM are not mutually exclusive. When jointly employing all of them(The final row), we can obtain the the best performance on all benchmarks.

6 Conclusions

In this work, we systematically analyze the limitations of DM algorithms under more complex and realistic domain shifts. We argue that the most popular method for domain adaptation - Distributional Matching relies on restrictive assumptions on underlying distributions and are usually not satisfied in real world. Thus we propose to replace matching distributions by matching discriminative patterns of predictors (PBs).

For quantitative analysis, we propose new RDS benchmarks and provide extensive empirical evaluations. To overcome these limitations and promote robust DA under RDS, we propose InstaPBM to match predictive behaviors across domains. Extensive experiments on both conventional and RDS benchmarks demonstrate the efficacy of InstaPBM. We hope our intuitive observations on DM methods and effective methods proposed in InstaPBM will serve as a new direction and achieve robust DA in real scenarios.

7 Broader Impact

Supervised learning algorithms suffer from low accuracy when the target test data is out of distribution of the source train data or lack of annotations. Domain adaptation (DA) is an actively researched area to solve this problem by leveraging the unlabeled target data and adapt the model to produce powerful predictions. In this work, we systematically analyze the limitations of the traditional distributional matching based design pattern for domain adaptation, discuss its flaws, and find it usually fails under real world domain shift. Such analysis will be helpful to avoid failures brought by the distributional matching based methods. To quantitatively verify the limitations of the distributional matching based methods, we propose new DA benchmarks with three types of Realistic Domain Shifts (RDS), which better reflect the real world scenarios and can promote DA research with more practical effectiveness. We propose a more intuitive and effective domain adaptation approach, which is closer to the essential human behavior and more robust to the real world scenarios. By achieving robust domain adaptation, our method can help machine learning model transfer the learned knowledge to new scenes. Since most distributional matching based DA methods suffer from instability in training and delicacy of special parameters, our proposed DA pattern are more robust, which is unquestionably more applicable in real industrial deployment. As for negative aspects, since the method is designed for unsupervised domain adaptation, it may not be able to achieve significant performance gain when there is several labeled samples in the target domain.

References

- [1] Hana Ajakan, Pascal Germain, Hugo Larochelle, François Laviolette, and Mario Marchand. Domain-adversarial neural networks. *arXiv:1412.4446*, 2014.
- [2] Tameem Adel, Han Zhao, and Alexander Wong. Unsupervised domain adaptation with a relaxed covariate shift assumption. In *AAAI Conference on Artificial Intelligence*, pages 1691–1697, 2017.
- [3] Yaroslav Ganin, Evgeniya Ustinova, Hana Ajakan, Pascal Germain, Hugo Larochelle, François Laviolette, Mario Marchand, and Victor Lempitsky. Domain-adversarial training of neural networks. *The Journal of Machine Learning Research*, 17(1):2096–2030, 2016.
- [4] Carlos J Becker, Christos M Christoudias, and Pascal Fua. Non-linear domain adaptation with boosting. In *Advances in Neural Information Processing Systems*, pages 485–493, 2013.
- [5] Muhammad Ghifary, W Bastiaan Kleijn, Mengjie Zhang, and David Balduzzi. Domain generalization for object recognition with multi-task autoencoders. In *IEEE International Conference on Computer Vision*, pages 2551–2559, 2015.
- [6] Xavier Glorot, Antoine Bordes, and Yoshua Bengio. Domain Adaptation for Large-Scale Sentiment Classification: A Deep Learning Approach. In *International Conference on Machine Learning*, pages 513–520, 2011.
- [7] Zhongyi Pei, Zhangjie Cao, Mingsheng Long, and Jianmin Wang. Multi-adversarial domain adaptation. In *AAAI Conference on Artificial Intelligence*, 2018.
- [8] Mingsheng Long, Yue Cao, Jianmin Wang, and Michael Jordan. Learning transferable features with deep adaptation networks. In *International Conference on Machine Learning*, pages 97–105, 2015.
- [9] I-Hong Jhuo, Dong Liu, DT Lee, and Shih-Fu Chang. Robust visual domain adaptation with low-rank reconstruction. In *IEEE Conference on Computer Vision and Pattern Recognition*, pages 2168–2175, 2012.

- [10] Judy Hoffman, Eric Tzeng, Taesung Park, Jun-Yan Zhu, Phillip Isola, Kate Saenko, Alexei A. Efros, and Trevor Darrell. Cycada: Cycle consistent adversarial domain adaptation. In *International Conference on Machine Learning*, 2018.
- [11] Sicheng Zhao, Bo Li, Xiangyu Yue, Yang Gu, Pengfei Xu, Runbo Hu, Hua Chai, and Kurt Keutzer. Multi-source domain adaptation for semantic segmentation. In *Advances in Neural Information Processing Systems*, pages 7285–7298, 2019.
- [12] Han Zhao, Remi Tachet Des Combes, Kun Zhang, and Geoffrey Gordon. On learning invariant representations for domain adaptation. In *International Conference on Machine Learning*, pages 7523–7532, 2019.
- [13] Yifan Wu, Ezra Winston, Divyansh Kaushik, and Zachary Lipton. Domain adaptation with asymmetrically-relaxed distribution alignment. *arXiv:1903.01689*, 2019.
- [14] Mingsheng Long, Zhangjie Cao, Jianmin Wang, and Michael I Jordan. Conditional adversarial domain adaptation. In *Advances in Neural Information Processing Systems*, pages 1640–1650, 2018.
- [15] Remi Tachet des Combes, Han Zhao, Yu-Xiang Wang, and Geoff Gordon. Domain adaptation with conditional distribution matching and generalized label shift. *arXiv:2003.04475*, 2020.
- [16] Antonio Torralba and Alexei A Efros. Unbiased look at dataset bias. In *IEEE Conference on Computer Vision and Pattern Recognition*, pages 1521–1528, 2011.
- [17] Bob L Sturm. A simple method to determine if a music information retrieval system is a “horse”. *IEEE Transactions on Multimedia*, 16(6):1636–1644, 2014.
- [18] Eric Tzeng, Judy Hoffman, Kate Saenko, and Trevor Darrell. Adversarial discriminative domain adaptation. In *IEEE conference on Computer Vision and Pattern Recognition*, pages 7167–7176, 2017.
- [19] Weixiang Hong, Zhenzhen Wang, Ming Yang, and Junsong Yuan. Conditional generative adversarial network for structured domain adaptation. In *IEEE Conference on Computer Vision and Pattern Recognition*, pages 1335–1344, 2018.
- [20] Zhenwei He and Lei Zhang. Multi-adversarial faster-rcnn for unrestricted object detection. In *IEEE International Conference on Computer Vision*, pages 6668–6677, 2019.
- [21] Rongchang Xie, Fei Yu, Jiachao Wang, Yizhou Wang, and Li Zhang. Multi-level domain adaptive learning for cross-domain detection. In *IEEE International Conference on Computer Vision Workshops*, 2019.
- [22] Xinge Zhu, Jiangmiao Pang, Ceyuan Yang, Jianping Shi, and Dahua Lin. Adapting object detectors via selective cross-domain alignment. In *IEEE Conference on Computer Vision and Pattern Recognition*, pages 687–696, 2019.
- [23] Yangtao Zheng, Di Huang, Songtao Liu, and Yunhong Wang. Cross-domain object detection through coarse-to-fine feature adaptation. *arXiv:2003.10275*, 2020.
- [24] Chen-Yu Lee, Tanmay Batra, Mohammad Haris Baig, and Daniel Ulbricht. Sliced wasserstein discrepancy for unsupervised domain adaptation. In *IEEE Conference on Computer Vision and Pattern Recognition*, pages 10285–10295, 2019.
- [25] Subhankar Roy, Aliaksandr Siarohin, Enver Sangineto, Samuel Rota Buló, Nicu Sebe, and Elisa Ricci. Unsupervised domain adaptation using feature-whitening and consensus loss. In *IEEE Conference on Computer Vision and Pattern Recognition*, pages 9471–9480, 2019.
- [26] Chao Chen, Zhihang Fu, Zhihong Chen, Sheng Jin, Zhaowei Cheng, Xinyu Jin, and Xian-Sheng Hua. Homm: Higher-order moment matching for unsupervised domain adaptation. *arXiv:1912.11976*, 2019.
- [27] Jiayuan Huang, Arthur Gretton, Karsten Borgwardt, Bernhard Schölkopf, and Alex J Smola. Correcting sample selection bias by unlabeled data. In *Advances in Neural Information Processing Systems*, pages 601–608, 2007.

- [28] Jian Shen, Yanru Qu, Weinan Zhang, and Yong Yu. Wasserstein distance guided representation learning for domain adaptation. In *AAAI Conference on Artificial Intelligence*, 2018.
- [29] Yann LeCun, Léon Bottou, Yoshua Bengio, Patrick Haffner, et al. Gradient-based learning applied to document recognition. *Proceedings of the IEEE*, 86(11):2278–2324, 1998.
- [30] Xingchao Peng, Qinxun Bai, Xide Xia, Zijun Huang, Kate Saenko, and Bo Wang. Moment matching for multi-source domain adaptation. In *IEEE International Conference on Computer Vision*, pages 1406–1415, 2019.
- [31] Yves Grandvalet and Yoshua Bengio. Semi-supervised learning by entropy minimization. In L. K. Saul, Y. Weiss, and L. Bottou, editors, *Advances in Neural Information Processing Systems 17*, pages 529–536. 2005.
- [32] Shuhao Cui, Shuhui Wang, Junbao Zhuo, Liang Li, Qingming Huang, and Tian Qi. Towards discriminability and diversity: Batch nuclear-norm maximization under label insufficient situations. *arXiv:2003.12237*, 2020.
- [33] Qizhe Xie, Zihang Dai, Eduard Hovy, Minh-Thang Luong, and Quoc V Le. Unsupervised data augmentation for consistency training. *International Conference on Learning Representations*, 2019.
- [34] Takeru Miyato, Shin-ichi Maeda, Masanori Koyama, and Shin Ishii. Virtual adversarial training: a regularization method for supervised and semi-supervised learning. *IEEE Transactions on Pattern Analysis and Machine Intelligence*, 41(8):1979–1993, 2018.
- [35] Hongyi Zhang, Moustapha Cisse, Yann N Dauphin, and David Lopez-Paz. mixup: Beyond empirical risk minimization. *arXiv preprint arXiv:1710.09412*, 2017.
- [36] Yu Sun, Eric Tzeng, Trevor Darrell, and Alexei A Efros. Unsupervised domain adaptation through self-supervision. *arXiv:1909.11825*, 2019.
- [37] Fabio M Carlucci, Antonio D’Innocente, Silvia Bucci, Barbara Caputo, and Tatiana Tommasi. Domain generalization by solving jigsaw puzzles. In *IEEE conference on Computer Vision and Pattern Recognition*, pages 2229–2238, 2019.
- [38] Yaroslav Ganin and Victor Lempitsky. Unsupervised domain adaptation by backpropagation. In *International Conference on Machine Learning*, pages 1180–1189, 2015.
- [39] Pablo Arbelaez, Michael Maire, Charless Fowlkes, and Jitendra Malik. Contour detection and hierarchical image segmentation. *IEEE Transactions on Pattern Analysis and Machine Intelligence*, 33(5):898–916, 2011.
- [40] Yuval Netzer, Tao Wang, Adam Coates, Alessandro Bissacco, Bo Wu, and Andrew Y Ng. Reading digits in natural images with unsupervised feature learning. In *Advances in Neural Information Processing Systems Workshops*, 2011.
- [41] Xingchao Peng, Ben Usman, Neela Kaushik, Judy Hoffman, Dequan Wang, and Kate Saenko. Visda: The visual domain adaptation challenge. *arXiv:1710.06924*, 2017.
- [42] Yaroslav Ganin, Evgeniya Ustinova, Hana Ajakan, Pascal Germain, Hugo Larochelle, François Laviolette, Mario Marchand, and Victor Lempitsky. Domain-adversarial training of neural networks. *Journal of Machine Learning Research*, 17(1):2096–2030, 2016.
- [43] Baochen Sun, Jiashi Feng, and Kate Saenko. Return of frustratingly easy domain adaptation. In *AAAI Conference on Artificial Intelligence*, pages 2058–2065, 2016.
- [44] Baochen Sun and Kate Saenko. Deep coral: Correlation alignment for deep domain adaptation. In *European Conference on Computer Vision Workshops*, pages 443–450, 2016.
- [45] Pietro Morerio, Jacopo Cavazza, and Vittorio Murino. Minimal-entropy correlation alignment for unsupervised deep domain adaptation. In *International Conference on Learning Representations*, 2018.

- [46] Mingsheng Long, Han Zhu, Jianmin Wang, and Michael I Jordan. Deep transfer learning with joint adaptation networks. In *International Conference on Machine Learning*, pages 2208–2217, 2017.
- [47] Kuniaki Saito, Yoshitaka Ushiku, Tatsuya Harada, and Kate Saenko. Adversarial dropout regularization. *arXiv:1711.01575*, 2017.
- [48] Geoffrey French, Michal Mackiewicz, and Mark Fisher. Self-ensembling for visual domain adaptation. *arXiv:1706.05208*, 2017.
- [49] Guoliang Kang, Lu Jiang, Yi Yang, and Alexander G Hauptmann. Contrastive adaptation network for unsupervised domain adaptation. In *IEEE conference on Computer Vision and Pattern Recognition*, pages 4893–4902, 2019.
- [50] Kuniaki Saito, Kohei Watanabe, Yoshitaka Ushiku, and Tatsuya Harada. Maximum classifier discrepancy for unsupervised domain adaptation. In *IEEE Conference on Computer Vision and Pattern Recognition*, pages 3723–3732, 2018.
- [51] Rui Shu, Hung H. Bui, Hirokazu Narui, and Stefano Ermon. A DIRT-T Approach to Unsupervised Domain Adaptation. *arXiv:1802.08735*, 2018.

Supplementary Material: Rethinking Distributional Matching Based Domain Adaptation

1 Theoretical Proof

Given a probability space (X, Σ_1, P) and a measurable space (X, Σ_2) , $f : \mathcal{X} \rightarrow \mathcal{Y}$ is a measurable map. Then f induces a probability measure on Y by $P(f^{-1}(\cdot))$, which we denote as the induced probability measure $f^*(P)$.

In probability theory, A probability space (X, P) is complete means all subsets of a zero-probability set are measurable. (X, P) is non-atomic, when for any event $A \subseteq X$ with $P(A) > 0$, there is a subset $B \subset A$, such that $P(A) > P(B) > 0$.

Then we have the following lemma:

Lemma 1.1. Assume (\mathbb{R}^n, P) and (\mathbb{R}^m, Q) are two non-atomic probability distributions on spaces, namely, P and Q are defined on Borel σ -algebras and are complete. Then there is a measurable mapping $f : \mathbb{R}^n \rightarrow \mathbb{R}^m$, such that $f^*(P) = Q$.

Proof. From probability theory, any Borel complete probability measures on \mathbb{R}^n are standard probability spaces [?]. And it is a celebrated result that all non-atomic standard probability spaces are isomorphic [?], namely there is an invertible mapping $f : \mathbb{R}^n \rightarrow \mathbb{R}^m$ such that $f^*(P) = Q$ and $f^{-1*}(Q) = P$. ■

$k \in \mathbb{N}$ is an positive integer. We denote $[k] = \{1, 2, \dots, k\}$. Consider two domains S, T , and we want to perform k -classification problem on both domains, namely we want to learn a mapping $\mathcal{X} \rightarrow [k]$, where \mathcal{X} denotes the pixel space. Assume in both domains, data generating distributions $p_S(x), p_T(x)$ can be partitioned into $2k$ disjoint closed¹ manifolds S_1, S_2, \dots, S_k and T_1, T_2, \dots, T_k , each manifold corresponds to a class in source and target domains, this is a common assumption [?]. Formally, we have the supports of the distributions satisfy $\text{Supp}(p_S(x)) \subseteq \cup_{i=1}^k S_i$, $\text{Supp}(p_T(x)) \subseteq \cup_{i=1}^k T_i$. For simplicity we also assume that $p_S(S_i) = p_T(T_i) = 1/k$, $\forall i \in \{1, 2, \dots, k\}$.

We assume there is a source domain feature representation $f_S : \cup_{i=1}^k S_i \rightarrow \mathcal{Z}$, where f_S maps each S_i to Z_i , namely $f_S(S_i) \subseteq Z_i$, and $\{Z_i\}_{i=1}^k$ are pairwise disjoint closed sets. So there is an induced probability measure $f_S^*(p_S)$ of $p_S(x)$ induced by the mapping $f_S : \cup_{i=1}^k S_i \rightarrow \mathcal{Z}$ on \mathcal{Z} , we denote this probability measure as $p_S(z) = f_S^*(p_S)$. There is a classifier on \mathcal{Z} which maps each Z_i to the class label i .

The function $f_S : \cup_{i=1}^k S_i \rightarrow \mathcal{Z}$ can be extended² to a global representation function $f : \cup_{i=1}^k (S_i \cup T_i) \rightarrow \mathcal{Z}$. We call such an extension a "domain adapting extension".

Since on $\cup_{i=1}^k T_i$, there is a probability measure $p_T(x)$, the mapping $f|_{\cup_{i=1}^k T_i} : \cup_{i=1}^k T_i \rightarrow \mathcal{Z}$ induces a probability measure $p_T(z)$. Distributional matching methods aims at minimizing the divergence between $p_S(z)$ and $p_T(z)$. A permutation $\tau : [k] \rightarrow [k]$ is a one-to-one mapping of $[k]$. We further

¹These sets are closed sets, they does not need to be "closed manifolds" in differential geometry.

²This is to say $f|_{\cup_{i=1}^k S_i} = f_S$.

assume that all distributions on \mathcal{X} and \mathcal{Z} are non-atomic and complete. There is a very reasonable assumption, since both images and their latent representations should be continuous distributions on some low dimensional manifolds. We prove the following theorem:

Theorem 1.1. Assume τ is an arbitrary permutation of $[k]$. For any source domain feature representation $f_S : \cup_{i=1}^k S_i \rightarrow \mathcal{Z}$ satisfying conditions mentioned above, there is a domain adapting extension $f : \cup_{i=1}^k (S_i \cup T_i) \rightarrow \mathcal{Z}$, such that the following two assumptions are satisfied:

- $f(T_i) \subseteq Z_{\tau(i)}, \forall i \in [k]$.
- $p_T(z) = p_S(z)$.

Roughly speaking, f can be viewed as the shared representation for both source and target domains. The theorem can be described as "for any wrong class label assignment τ , there is a perfect distributional matching that wrongly maps true target domain labels to the wrong class label assignment."

Proof. For any label $i \in [k]$, we denote the data distribution with label i in both domains as $p_S^i(x), p_T^i(x)$. We can see that $\text{Supp}(p_S^i(x)) \subseteq S_i$, and $\text{Supp}(p_T^i(x)) \subseteq T_i$. Also, we denote $p_S^i(z) = f_S^*(p_S^i(x))$ the induced probability measure $f_S^*(p_S^i(x))$ of $p_S^i(x)$ by f_S on \mathcal{Z} . We can easily verify $\text{Supp}(p_S^i(z)) \subseteq Z_i$. Given a permutation τ , for all $i \in [k]$, one can verify the condition of lemma 1 holds:

- Both $(p_T^i(x), T_i)$ and $(p_S^{\tau(i)}, \mathcal{Z})$ are defined on real Euclidean spaces.
- Both $(p_T^i(x), T_i)$ and $(p_S^{\tau(i)}, \mathcal{Z})$ are Borel, complete and non-atomic.

So we can conclude that there is a function $f_T^i : T_i \rightarrow \mathcal{Z}$, such that $f_T^{i*}(p_T^i) = p_S^{\tau(i)}(z)$. Since $\text{Supp}(p_S^{\tau(i)}(z)) \subseteq Z_{\tau(i)}$, so by re-arranging a zero-probability set, one can let $f_T^i(T_i) \subseteq Z_{\tau(i)}$.

We define $f : \cup_{i=1}^k (S_i \cup T_i) \rightarrow \mathcal{Z}$ by $f|_{T_i} = f_T^i$ and $f|_{S_i} = f_S$ for all $i \in [k]$. From the above argument we can conclude that $f(T_i) \subseteq Z_{\tau(i)}, \forall i \in [k]$.

On the other hand, $p_T(z) = \sum_{i=1}^k p(\text{label} = i) p_T(z|\text{label} = i) = 1/k \sum_{i=1}^k p_S(z|\text{label} = \tau(i)) = p_S(z)$. So we can conclude such f satisfies the two conditions in the theorem. ■

2 Realistic Domain Shift Benchmarks

In this section, we provide the details of the proposed realistic domain shift (RDS) benchmarks. RDS benchmarks will be made available at [InstaPBM-RDS](#) once upon acceptance. We specify the statistics of each RDS benchmark and manifest how we create it based on existing DA benchmarks below.

2.1 Proposed benchmarks with Label Distribution Shift (LDS)

LDS indicates the mismatch of source and target label distributions. We create **Digits5-LDS**, **VisDA2017-LDS** and **DomainNet-LDS** based on Digits5 [? ? ? ?], VisDA2017 [?] and DomainNet [?] by re-sampling the target domain into long-tailed distributions among all classes while keep source domain unchanged. This is aligned with the realistic scenarios where the class labels of target domain are usually long-tail distributed. We first sort the labels by the number $l_i, i \in [0, L]$ (L is the amount of categories) of corresponding data in reverse order. Then we keep the order and sample a also reversely sorted sequence $\{s_0, \dots, s_i, \dots, s_L \mid s_i \in (0, 1), s_0 > s_1 > \dots > s_L\}$ from a power-law distribution, which need to be normalized to $(0, 1]$. We then use the sequence to randomly select target samples for each class by $\tilde{l}_i = s_i \cdot l_i$. Through this process, we do not make any increase to the source domain data and only remove certain amount of target samples. We illustrate LDS by each dataset in Fig. 1, Fig. 2, and Fig. 3.

2.2 Proposed benchmarks with Intermediate Layer Distribution Shift(ILDS)

ILDS indicates the intra-class feature distributions shift, which means that even with same semantic meaning, the proportion of sub-types could be hugely different across domains. Here we construct

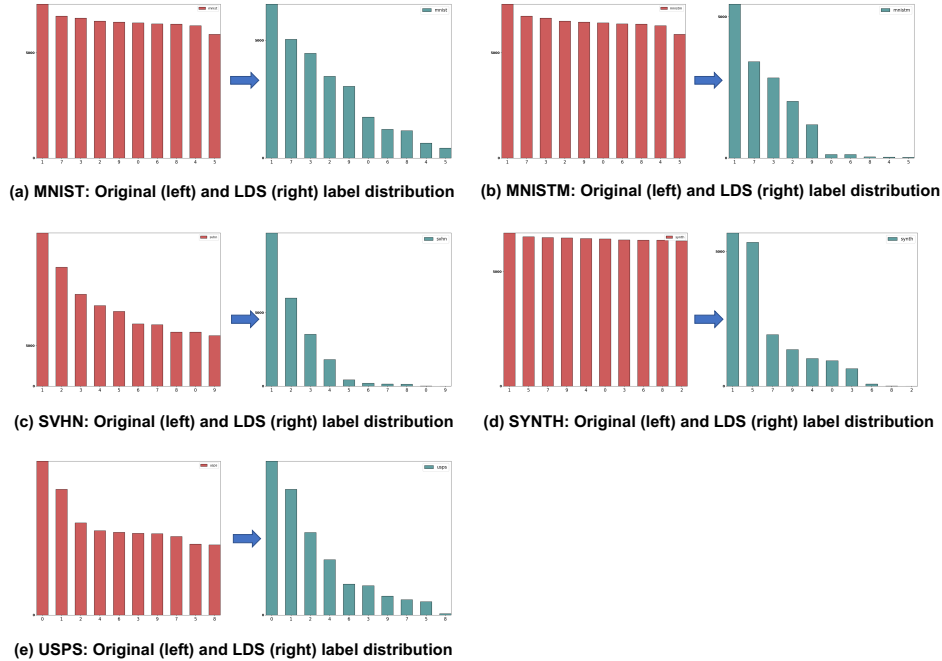


Figure 1: Label distributions of the proposed Digits5-LDS benchmarks. Please zoom for better view.

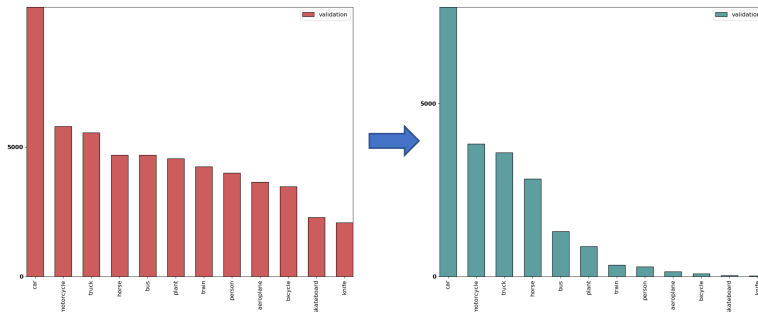


Figure 2: Label distributions of the proposed VisDA2017-LDS benchmark. Left: original label distribution; Right: LDS label distribution. Please zoom for better view.

DomainNet-ILDS based on the public DA benchmark DomainNet [?], since it contains 345 categories of common objects for each domain, and it splits 345 categories into 24 meta-categories (e.g. they conclude *alarm clock* and *candle* both into a common meta-label *office*). DomainNet inherently conforms to our assumption about ILDS, so we can create the sub-label distribution shift for each meta-label between domains. Similar with the process in Sec. 2.1, we sort the sub-labels by the amount $l_i^k, i \in [0, L_k]$ of corresponding data in reverse order for each specific meta-label k (L_k denotes the specific number of sub-labels corresponding to the meta-label k). Then, we individually create a reversely sorted sequence $\{s_0^k, \dots, s_i^k, \dots, s_{L_k}^k \mid s_i^k \in (0, 1), s_0^k > s_1^k > \dots > s_{L_k}^k\}$ from a power-law distribution for each meta-label k . Finally, we select target samples according to $\tilde{l}_i^k = l_i^k \cdot s_i^k, i \in [0, L_k]$ for the corresponding data subset of each meta-label k . We illustrate the details of sub-label distribution in Fig. 4, where each color denotes each meta-label.

2.3 Proposed Target with Outliers (TwO) benchmark

TwO indicates the target domain contains samples that lie outside the support of the source domain. To create such benchmark, we choose ImageNet 1K[?] as the source domain and DomainNet [?] as

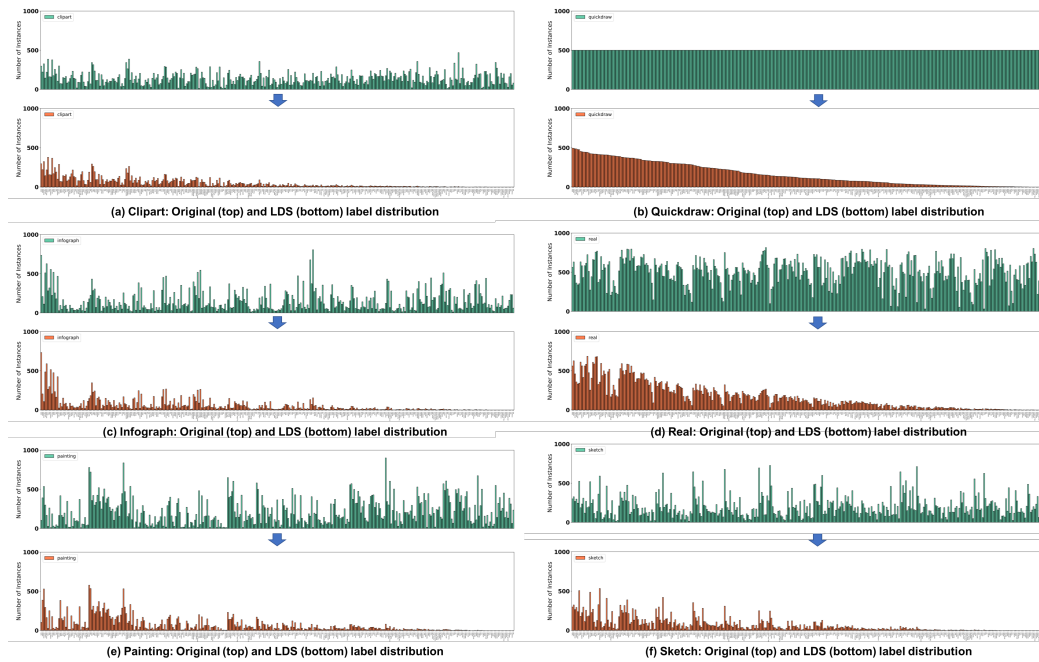


Figure 3: Label distributions of the DomainNet-LDS benchmarks. Please zoom for better view.

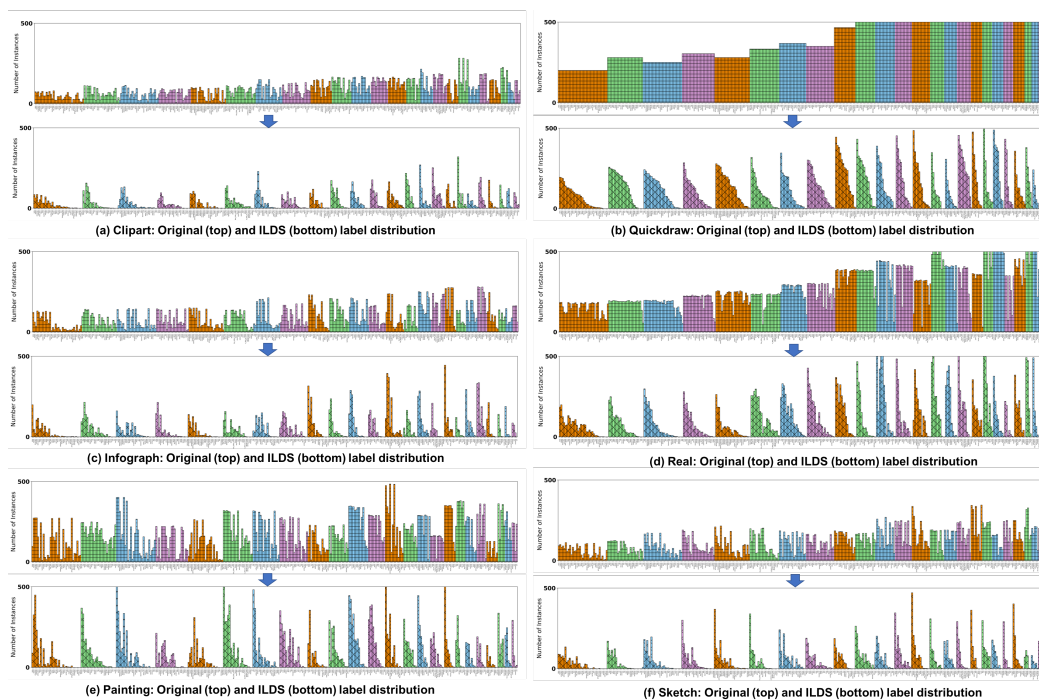


Figure 4: Label distributions of the DomainNet-ILDS benchmarks. Please zoom for better view.

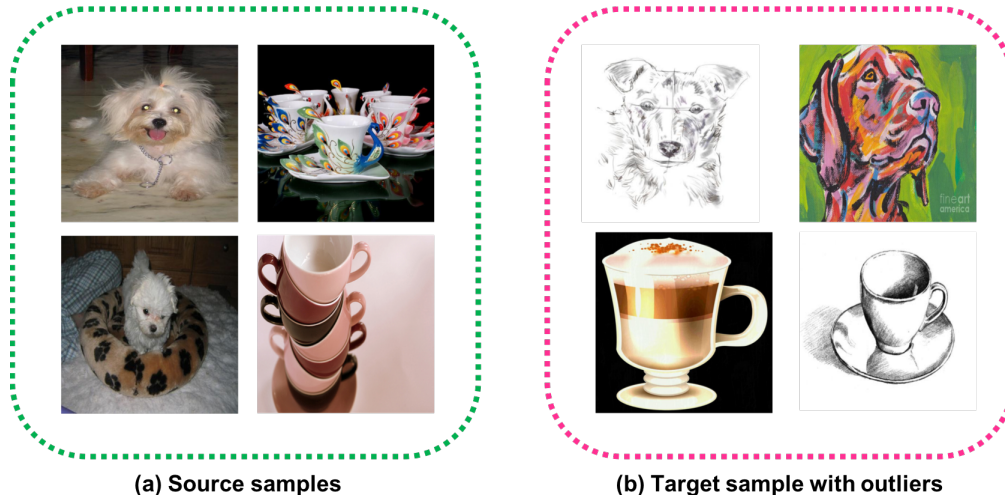


Figure 5: Source and target samples of the proposed TwO benchmarks

the target domain. We select 18 overlapping categories from these two datasets to ensure the source and target domains share the same set of classes. We add noisy examples (outliers) by sampling from each domain in DomainNet. For example, *dog* from source domain (ImageNet) are mostly from natural scenes while *dog* from target domain (DomainNet) are collected from 6 domains (Clipart, Inforgraph, Real, Painting, Sketch, Quickdraw) which are hugely diverse from the source domain. In this setting, TwO reflects the problems in the real world, because the model may see a variety of objects with the same semantic meaning but in different visual appearances. We illustrate the details from an example in Fig. 5.

3 Methodological Details

In the main body of our paper, we have proposed three major predictive behaviors matching mechanisms on both source and target domains, and one additional predictive behavior matching mechanism that has been introduced by other works, which can also be induced into our general adaptation pattern(i.e. PBM). Nevertheless, due to the limitation of space, we do not offer much implementation details of these components. Thus, we elaborate them comprehensively in this section.

In each iteration step, we randomly take two samples $(x_s, y_s), (x_t)$ from source domain and target domain respectively (For simplicity, we take the batch size being 2 as an example. This setting can be easily generalized to those scenarios where batch size is larger than 2). Then by applying semantic preserving \mathcal{T}_{sp} operations twice on each sample, we can get two extra data tuples: $(x_s^{sp}, y_s), (x_t^{sp})$. Besides, we denote the model’s predicted results of each sample as $p_\theta(y|x_s), p_\theta(y|x_t), p_\theta(y|x_s^{sp}), p_\theta(y|x_t^{sp})$ with regard to $x_s, x_t, x_s^{sp}, x_t^{sp}$, respectively.

3.1 Mutual Information Predictive Behavior Matching

First, by calculating the supervised loss $\mathcal{L}_M(S; \theta) = \mathcal{L}_X(y_s, p_\theta(y|x_s)) + \mathcal{L}_X(y_s, p_\theta(y|x_s^{sp}))$ where \mathcal{L}_X denotes the cross entropy loss, we supervisedly train the model on source domain, which will maximize the mutual information between x_s and y_s . To make the model also keep this predictive behavior on target domain, we calculate the MI loss $\mathcal{L}_M(T; \theta)$ on target samples. Specifically, as mentioned in Sec. 4.1 of the main paper, $\mathcal{L}_M(T; \theta)$ consists of two part:

$$\mathcal{L}_M(T; \theta) = \mathbb{E}_{y \sim \mathcal{P}_\theta(Y)} [\log p_\theta(y)] - \mathbb{E}_{x_t \sim \mathcal{P}_T(X)} [\sum_y p_\theta(y|x_t) \log p_\theta(y|x_T)] \quad (1)$$

The second part is exactly the objective of minimizing the conditional entropy, which can be easily calculated directly based on the formulation. However, when it comes to the implementation of the first part(i.e. info-entropy $H(Y)$ maximization), it seems not intuitive enough. The obstacle here is that we need to get the specific distribution $\mathcal{P}_\theta(Y)$ of predicted target label y in order to get the

probability $p_\theta(y)$. It requires us to access all predictions across the whole target domain’s samples in each iteration, which is impractical. The most obvious solution is resorting to Monte-Carlo estimation of $\mathcal{P}_\theta(Y)$ by only using a mini-batch of data. However, this requires the batch size to be as large as possible in order to obtain a good estimation, which we can not satisfy, because the larger the batch size, the more GPU resources we need to use. Here, we adopt an alternative to keep a global moving average $q(y)$ as an approximation of $p_\theta(y)$. To be more specific, we maintain a size-fixed stack during training. The stack are used to save the most recent K predicted results of x_t so that we can estimate $q(y)$ via calculating the distribution of these results. Then the gradient of $\mathbb{E}_{y \sim \mathcal{P}_\theta(Y)}[\log p_\theta(y)]$ as $\sum_{(x,y) \sim \mathcal{P}_S} \nabla_{\theta} p_\theta(y|x) \log q(y)$ can be estimated. Therefore, we can match the mutual information predictive behavior on both domains by optimizing the loss:

$$\mathcal{L}_M(S, T; \theta) = \mathcal{L}_M(S; \theta) + \mathcal{L}_M(T; \theta) \quad (2)$$

3.2 Contrastive Predictive Behavior Matching

As discussed in Sec. 4.2 of the main paper, the objective of Contrastive Predictive Behavior Matching (CPBM) can be written as:

$$\begin{aligned} \mathcal{L}_C(S, T; \theta) = & \mathbb{E}_{x \sim \mathcal{P}_{S, T}, t \sim \tau} [D_{KL}(p_\theta(y | x) || p_\theta(y | t(x)))] \\ & - \lambda_{con} \mathbb{E}_{(x,y) \sim \mathcal{P}_S, (x',y') \sim \mathcal{P}_S, y \neq y'} [D_{KL}(p_\theta(y | x) || p_\theta(y' | x'))] \end{aligned} \quad (3)$$

where $\mathcal{P}_u, u \in \{S, T\}$ denotes the distribution of domains, λ_{con} denotes a trade-off term between two contrastive items. The goal of the first term is to add a locally-smoothness constraint via minimizing the divergence between a sample and its vicinity. According to [?], this constraint play an rather important role in the effectiveness of the second part of Eq. 1(i.e. Conditional Entropy Minimization). Following [?], the first item can be readily implemented by calculating the KL divergence $D_{KL}(p_\theta(y|x_s), p_\theta(y|x_s^{sp}))$ and $D_{KL}(p_\theta(y|x_t), p_\theta(y|x_t^{sp}))$ in each iteration. The second term aims to maximize divergence between samples belonging to different classes. In practice, we will randomly sample another datapoint $(x'_s, y'_s), s.t. y'_s \neq y_s$ from source domain in addition to (x_s, y_s) and get the predicted probability vector $p_\theta(y|x'_s)$ through the classification model, then calculate the KL divergence between $p_\theta(y|x'_s)$ and $p_\theta(y|x_s)$.

3.3 Mix-up Predictive Behavior Matching

As for the implementation of Mix-up predictive behavior matching (MuPBM), we also randomly sample two new samples (x''_s, y''_s) and (x''_t) in addition to $(x_s, y_s), (x_t)$. Then we generate the new mixed samples $(\tilde{x}_s = \beta x_s + (1 - \beta)x''_s, \tilde{y}_s = \beta y_s + (1 - \beta)y''_s)$ and $(\tilde{x}_t = \beta x_t + (1 - \beta)x''_t)$ where $\beta \in [0, 1]$. For the sample from the source domain, we directly calculate the KL divergence between the predicted probability vector $p_\theta(y|\tilde{x}_s)$ and the one-hot vector \tilde{y}_s . For the sample from the target domain, we use an estimated alternative $\tilde{y}_t \approx \beta p_\theta(y|x_t) + (1 - \beta)p_\theta(y|x''_t)$ and then calculate the KL divergence between $p_\theta(y|\tilde{x}_t)$ and \tilde{y}_t . The goal of MuPBM is to minimize these two KL divergences. The intuition of this objective is to ensure a smooth transition between classes and encourages the model to behave similarly on linear interpolations of samples in both domains.

3.4 Other Predictive Behavior Matching

In Sec. 4.4 of the main paper, we briefly introduce the Task-oriented predictive behavior matching. Following [?], each pretext task shares the same feature encoder to obtain the same latent representations while we assign a task-specific head to each task. We denote the feature encoder as $g(\cdot)$ and the task-specific heads as $h_{rot}(\cdot), h_{qdr}(\cdot), h_{flip}(\cdot)$, corresponding to three pretext tasks Rotation Prediction, Patch Location Prediction, and Vertical Flip Prediction, respectively. In practice, we generate new task-specific samples $\{(x_u^{sp}, y_u^{sp}) | sp \in [rot, qdr, flip], u \in [s, t]\}$ through transformation operation \mathcal{T}_{st} from x_s, x_t . Then we optimize the task-specific losses $\{L_{sp}(h_{sp} \circ g(x_u^{sp}), y_u^{sp}) | sp \in [rot, qdr, flip], u \in [s, t]\}$. It is worth noting that these pretext optimization objectives are domain agnostic which guarantees that this predictive behavior is matched in source and target domains.

So far, we have elaborated the implemental details of four different types of predictive behavior matching losses. In the end, we sum them up and update the network by minimizing the weighted combined loss.

Table 1: Performance comparison of the proposed InstaPBM and state-of-the-art UDA approaches on **VisDA2017-LDS** Benchmarks based on ResNet-101. The best accuracy is emphasized in bold.

Method	a-plane	bicycle	bus	car	horse	knife	m-cycle	person	plant	skb	train	truck	Average
Source Only	74.6	11.5	68.8	97.1	58.1	13.3	85.5	11.0	95.5	23.9	83.5	31.3	54.5
DAN [?]	66.3	7.2	60.9	88.1	42.6	9.8	77.1	4.5	82.0	15.4	75.5	27.7	46.4
DANN [?]	67.3	10.5	56.8	84.5	33.2	12.5	83.4	7.6	89.4	20.7	71.5	33.4	47.6
CoRAL [?]	67.5	18.7	63.7	84.2	32.3	28.5	70.1	9.1	82.3	24.6	76.9	36.5	49.5
HoMM [?]	70.8	17.3	64.2	88.3	30.7	20.7	83.7	14.5	91.7	25.3	73.5	40.7	51.8
JAN [?]	69.8	12.8	56.4	85.4	54.3	16.7	74.6	9.8	86.6	26.3	78.6	25.8	52.6
sDANN- β [?]	73.4	30.7	64.2	89.2	57.8	36.7	80.5	24.3	87.2	37.5	84.9	43.2	59.1
CDAN [?]	85.3	57.9	81.2	59.5	67.3	54.5	80.2	52.3	84.9	41.2	75.5	33.2	64.4
CDAN+E [?]	86.7	60.6	83.4	73.7	71.6	50.5	84.4	60.9	88.3	40.0	82.7	25.5	66.5
CAN [?]	88.6	65.4	75.3	88.3	80.9	53.5	88.9	64.7	79.5	69.4	73.1	32.6	71.7
ADR [?]	75.3	50.5	90.1	83.9	75.4	60.5	78.5	69.0	90.1	34.5	79.3	30.2	68.1
SE [?]	86.5	53.3	79.5	76.3	91.2	85.3	76.5	80.1	85.5	42.1	75.0	38.5	72.1
InstaPBM(ours)	87.3	67.5	83.2	74.8	91.8	61.3	88.4	72.7	87.3	59.5	85.0	45.5	74.5

Table 2: Performance comparison of the proposed InstaPBM and state-of-the-art UDA approaches on **Digits5-LDS** Benchmarks. The best accuracy is emphasized in bold.

Method	MN				MM				US				SY				SV				Average
	MM	US	SY	SV	MN	US	SY	SV	MN	MM	SY	SV	MN	MM	US	SV	MN	MM	US	SY	
Source Only	64.4	65.9	38.5	38.9	91.8	69.6	49.4	22.1	50.7	29.9	27.4	25.6	87.3	62.5	84.6	76.5	57.0	45.2	58.7	70.5	55.8
DAN [?]	59.9	44.7	30.7	16.2	76.3	51.4	47.3	41.9	73.7	28.0	28.3	18.2	64.6	56.5	51.5	68.6	43.9	41.6	36.2	62.4	47.1
CoRAL [?]	67.5	83.0	30.0	11.7	87.5	72.5	46.5	26.9	44.6	30.2	24.5	6.2	63.8	47.4	62.6	68.2	43.9	39.7	40.5	61.0	47.9
DANN [?]	63.3	53.2	32.4	20.6	79.2	58.2	46.6	36.1	79.7	41.2	31.6	21.9	70.9	53.1	61.4	71.0	40.5	35.7	37.1	68.5	50.1
HoMM [?]	64.6	59.4	37.8	20.7	82.0	66.0	49.1	31.7	69.6	31.8	27.7	21.0	68.1	58.0	67.2	67.6	42.6	39.1	35.9	69.6	50.5
JAN [?]	61.1	70.2	38.5	31.6	81.2	73.2	41.3	22.2	57.3	36.4	30.6	25.5	82.7	53.8	67.9	70.3	41.3	42.0	48.5	72.5	52.4
CDAN [?]	64.2	60.2	37.6	27.1	85.7	70.4	51.5	34.9	66.6	31.9	29.2	22.2	81.5	63.7	75.8	71.9	47.3	43.7	46.9	76.1	54.4
CDAN+E [?]	60.5	61.7	31.9	30.9	79.4	77.9	51.3	30.1	83.9	24.1	26.0	23.6	90.8	58.7	87.9	74.5	50.0	41.0	67.0	80.4	56.6
CAN [?]	67.9	76.5	42.4	38.5	99.6	79.7	60.6	25.2	34.7	34.4	27.0	20.2	88.4	65.2	78.6	83.0	45.6	52.2	69.2	78.4	58.4
ADR [?]	78.3	77.3	46.7	29.6	95.0	73.1	52.0	33.9	34.0	31.6	27.5	26.3	82.3	65.6	82.3	74.5	64.9	45.4	53.3	74.7	57.5
SE [?]	77.9	81.2	41.6	28.4	90.7	80.4	61.3	41.3	75.3	43.2	36.8	31.2	75.0	61.2	80.1	84.5	59.8	52.3	57.5	81.1	62.1
InstaPBM(ours)	82.9	75.3	49.4	45.9	92.1	72.4	53.7	49.6	81.1	50.0	42.7	45.2	90.0	67.6	82.7	79.3	59.0	51.4	72.3	80.5	66.2

4 Experimental Details

4.1 Implementation Details and Hyperparameter Tuning

We use mini-batch stochastic gradient descent (SGD) with momentum of 0.9 and weight decay of $5e-4$ to train the network. For benchmarks on Digits5, we use LeNet as backbone network and replace the last fully-connected(FC) layer with task-specific FC layer. We set initial learning rate as 0.1 and batch size as 512. The total training epochs are 45. Moreover, all the input images are resized into 32×32 . For benchmarks on VisDA2017, we use the pretrained ResNet101 as backbone network and also replace the last fully-connected(FC) layer with task-specific FC layer. The initial learning rate is $1e-4$ and batch size is 32. We set total epochs as 50. Besides, all input images are resized into 256×256 . We conduct all the experiments based on pytorch version 1.1 with CUDA version 10.1. The specific GPU type we used is Tesla P40. Moreover, there are 5 hyperparameters in our methods, which are λ_M for MIM loss, λ_C, λ_{con} for CPBM loss, λ_U for MuPBM loss and λ_S for TPBM loss. In all experiments, we fixed $\lambda_M = 1, \lambda_C = 0.1, \lambda_{con} = 0.1, \lambda_U = 0.01, \lambda_S = 0.1$. Codes will be available at anonymous link: [InstaPBM-RobustDA](#).

4.2 More Results and Analysis

Due to the space limitation of the main paper, we provide the results and analysis of the Label Distribution Shift Benchmarks, Digits5-LDS Benchmark and VisDA2017-LDS Benchmark, in this section. In fact, more and more recent novel works[? ? ?] suggest that the class-agnostic distributional matching methods seriously suffer from LDS. The specific reasons have been analyzed in Sec. 2 of the main paper. Here we can briefly state this issue from a more intuitive perspective according to [?]. Considering the optimal scenario of distributional matching where we have perfectly matched the representations \mathcal{Z}_s and \mathcal{Z}_t from different domains. Then we have $\mathcal{P}(\mathcal{Z}_s) = \mathcal{P}(\mathcal{Z}_t)$.

Because the classifier $h(\cdot)$ is a deterministic function, $\mathcal{P}(\mathcal{Z}_s) = \mathcal{P}(\mathcal{Z}_t)$ will lead to the consequence that $\mathcal{P}(h(\mathcal{Z}_s)) = \mathcal{P}(h(\mathcal{Z}_t))$, which only performs well when the label distributions are aligned between source and target domains.

Similar with the table’s layout In Sec. 5 of the main paper, the Table 2 and Table 1 are composited with three main clusters as well, which are, DM based methods (DAN, DANN, CoRAL, HoMM), conditional DM based methods (JAN, CDAN, CAN), and none DM methods (ADR, SE, InstaPBM). Both tables show the general trend that, when the Label Distribution Shift is serious, none DM methods outperform conditional DM methods while conditional methods outperform DM methods. In particular, our InstaPBM obtains 10.4% and 4.1% performance gain on Digits5-LDS Benchmark as compared to the results of Source Only and the best baseline (i.e. SE), respectively. Besides, our InstaPBM obtains 20.0% and 2.4% performance gain on VisDA2017-LDS Benchmark as compared to the results of Source Only and the best baseline (i.e. SE), respectively.

Most DM based methods, like DAN, CoRAL, DANN, are even worse than the results obtained by training on source only, which indicates that when the Label Distribution Shift is rather serious, the DM based methods even impair the domain adaptation process instead of promoting it. Since results on three different LDS Benchmarks (Digits5-LDS, VisDA2017-LDS, DomainNet-LDS) all show the akin phenomenon, we can modestly draw the conclusion that, at the very least, the performance of DM methods has a negative correlation with the extent of LDS. This is aligned with our analysis in Sec.2 of the main paper.